New calculation methods of diurnal distribution of solar radiation and its interception by canopy over complex terrain

Shusen Wang, Wenjun Chen, and Josef Cihlar

Natural Resources Canada,
Canada Centre for Remote Sensing,
Ottawa, Canada

Submitted to: **Ecological Modelling**, volume 155, number 2, 2002

Abstract

The prescription of diurnal radiation distribution and the consideration of topographic impact on canopy radiation interception are often required in ecological modelling studies. The most commonly used methods in current models are the sine-curve assumption for diurnal radiation distribution and the topographic geometric projection for canopy radiation interception. In this study, the defects of these two methods are examined and two new methods are proposed. The new method for prescribing the diurnal radiation distribution is based on the assumption that the direct normal radiation and diffusive radiation follow the sine-curve of solar zenith angle. This improvement is particularly important to the modelling strategies of separating canopy leaves into sunlit and shaded. It can also be used to extrapolating daily data to hourly values so that the short time step models can be applied when only daily data are available. The new method for calculating canopy radiation interception over inclined surfaces is based on the hypothesis that the topographic variation of canopy radiation interception is caused by the variation of sunlit/shaded leaf area index. This new method gives the same amount of total radiant energy interception as the geometric projection method, but it may lead to very different impact of topography on ecological processes. The topographic variation of canopy photosynthesis was investigated by using this new approach and compared with that obtained by using the direct geometric projection method. The two new approaches proposed in this study are more physically realistic in regenerating the natural processes. The improvements can benefit ecological models on temporal integration studies as well as spatial scale analysis over complex terrain.

Keywords: radiation; ecological model; complex terrain; topography; photosynthesis

1 Introduction

Modelling studies of the terrestrial ecosystems at large spatial and temporal scales frequently face two difficulties in practice: data availability and trade-off between high and low temporal or spatial resolutions. While physical and physiological processes of ecosystems can be studied in details using short time step models (e.g., half-hourly, Wang et al., 2001, 2002), the requirement of intensive data inputs and high demand of computing time often hinders their direct applications to the large scale studies. Models developed at longer time steps (e.g., daily, Running and Coughlan, 1988; Liu et al, 1997; or monthly, Parton et al., 1987; McGuire et al., 1997) are easier to be applied to the large scale studies. However, they are subject to the limitations of implementing mechanistically based processes and the loss of model sensitivity to environmental conditions. In addition, the non-linear relationships between model inputs and outputs are inherent to most ecosystems, such as the hyperbolic relationship between radiation and photosynthesis commonly used in modelling applications. Using average values of time dependent parameters and driving variables in low temporal resolution models runs a risk of biased model predictions.

The same limitations also exist when models are applied at low spatial resolutions, such as the land surface schemes coupled with general circulation models (~1°). Land surfaces often show very well-pronounced heterogeneity in the factors that control modelled processes. Current methods in model regional applications are using the pixel arithmetically averaged or representative parameters and driving variables as model inputs. Again, due to the non-linear relationships of model inputs and outputs and the loss of landscape variations that exist below the resolution, biased model predictions may occur. Increase of spatial resolution can reduce the risk, but it is also limited by data availability and over loading of computing time.

Attempts in addressing the temporal resolution problems have been made in some models. For example, BEPS (Liu et al., 1997) is a daily time step model developed for evaluating forest ecosystem productions at regional scale. Instead of using daily means of radiation directly for photosynthesis calculations, BEPS uses a daily integration method through which some important variations within the running time step can be captured (Chen et al., 1999). Similar modelling strategy that calculates photosynthesis at a daily time step but considering the diurnal variations of solar radiation can also be found in Hanson (1991), Sands (1995), and Liu (1996). One main assumption used by these models is the sine- (or cosine-) curve distribution of diurnal solar radiation. The accuracy of radiation prescription is important because it determines the main modelled processes. For example, in BEPS (Chen et al., 1999), the radiation curve is used to complete the temporal integration of Farquhar's photosynthesis model; it not only determines the estimated radiation at noon which is an important variable in calculating stomatal resistance and thereafter transpiration, it also controls the modelled radiation incident on sunlit leaves which affects leaf photosynthesis calculations.

The effects of using different spatial resolutions on model predictions have also been investigated by some authors. Band (1993) found that under dry conditions, aggregating the landscape from cell sizes of 30 m up to 1 km had significant effects on the areal carbon and water flux estimations over a strongly heterogeneous mountain basin. By running the FOREST-BGC model at different spatial resolutions ranging from 1 km up to 1°, Pierce and Running (1995) estimated that averaging sub-grid landscape variations typical of the northern US Rocky Mountains could result in overestimates of net primary production (NPP) as large as 30%. In another study using the SiB model and FIFE data, Sellers et al. (1997) explored the impact of area-averaging initial or boundary conditions of topography, vegetation and soil moisture at

30×30 m^2 resolution on the modelled ecosystem-atmosphere heat and water fluxes at a scale of 10 km^2. It was found that simple averages of topographic slopes and vegetation parameters can be used to calculate surface heat and water fluxes over a wide range of spatial scales, from a few meters up to many kilometres, to within an acceptable accuracy for climate modelling studies.

Radiation is one of the main driving variables in ecosystem energy, water and carbon processes. Reliable calculations of surface radiation data are a basic requirement for ecological models at any temporal and spatial scale. In this paper, two new methods in radiation calculations are proposed which can be used in addressing the above temporal and spatial resolution issues in ecological models. First, we propose a new scheme for prescribing the diurnal variations of solar radiation. It is mainly based on the assumption that the diurnal variation of direct normal radiation (direct radiation received on a surface normal to the rays from the sun) follows the sine-curve of solar zenith angle, rather than that received on a horizontal surface which is commonly used in most modelling applications. We found this new prescription is more physically realistic and accurate. This differentiation is important particularly to the modelling strategy of separating canopy leaves into sunlit and shaded. Second, we propose a new scheme for the calculations of radiation interception by forest canopy over inclined land surfaces such as complex mountainous terrain. It is recognised that the direct radiation intensity incident on leaf surface does not change with topographic slopes and aspects (when the land surface is not shaded) because trees always tend to grow up straight. The relative positions between plant leaves and the solar beam always tend to keep the same no matter what kinds of terrain the trees grow on. In our new modelling scheme, the topographic change of total radiant energy intercepted by canopy is attributed to the variation of the "path quality" of the solar beam within the canopy, which leads to the change of plant sunlit/shaded leaf area. Canopy

photosynthesis modelled by the new scheme can be substantially different from that by the direct geometrical projection method. After the two new methods are introduced, model experiment and comparisons are conducted and results are analysed.

2 Model description

2.1 Diurnal distribution of solar radiation

2.1.1 Problems with the current calculation methods

The following sine-curve assumption has been widely used in ecological models to prescribe the diurnal distribution of solar radiation from its daily means (Monteith, 1965; Hanson, 1991; Sands, 1995; Liu, 1996)

$$S = S_n \sin(\frac{\pi t}{D}) = \frac{\pi S_{day}}{2} \sin(\frac{\pi t}{D}) \tag{1a}$$

where S is the instantaneous solar radiation on a horizontal surface, S_n is S at noon, t is time, D is day length, and S_{day} is the daily mean of S. The relationship of $S_n/S_{day}=\pi/2$ is obtained by integrating Eq.(1a) with time ($0\le t\le D$) in a day. Another form of this equation used by some authors (Chen et al., 1999) is to assume S changes with solar zenith angle θ instead of time t as in Eq. (1a), which is written as

$$S = S_n \cos(\frac{\theta - \theta_n}{\pi/2 - \theta_n} \frac{\pi}{2}) = \frac{\pi S_{day}}{2} \cos(\frac{\theta - \theta_n}{\pi/2 - \theta_n} \frac{\pi}{2}) \tag{1b}$$

where θ_n is θ at noon. The relationship of $S_n/S_{day}=\pi/2$ is obtained by integrating Eq.(1b) with θ ($\pi/2\le\theta\le\theta_n$) in a day. Given the day of year DOY=150 at our study site (latitude ϕ=47.3°) as an example in which θ_n=25.5° and D=15.4h, the result produced by Eq. (1a) and Eq. (1b) is represented by curve *a* and curve *b*, respectively, in Fig. 1.

We found through close examinations on the above assumptions that both Eq. (1a) and Eq. (1b) not only have limitations in the prediction accuracy (discussed in Section 3.1), they also

cause serious problems in some model applications. For example, recent development of ecological models tends to separate the canopy leaves into sunlit and shaded categories which is found to provide a considerable advantage and improvement in the scale-up calculations of photosynthesis from leaf to canopy (Sinclair and Knoerr, 1982; Boote and Loomis, 1991; Wang et al., 2001). To estimate the sunlit leaf irradiance, we first need to calculate the radiation on a surface normal to the rays from the sun – the normal radiation S_s. With the assumption of Eq. (1a) and Eq. (1b), it can be obtained by

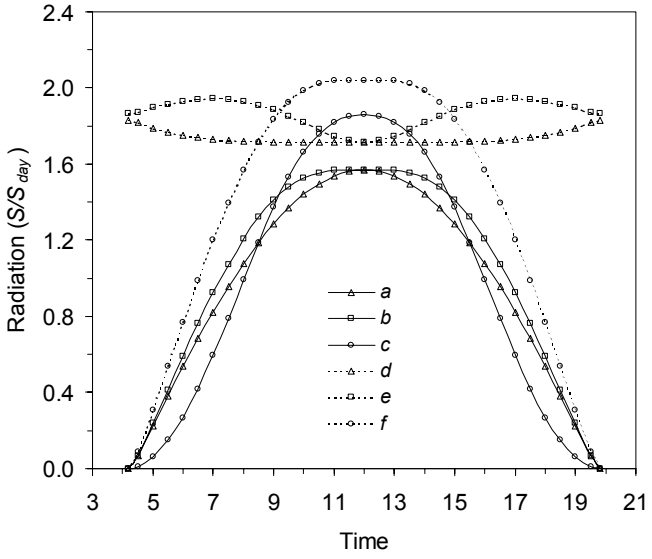

Figure 1. Diurnal distribution of solar radiation predicted by the sine-curve methods of Eq. (1a) (curve *a*) and Eq. (1b) (curve *b*) and the method of this study (curve *c*). Curves *d*, *e*, and *f* are the corresponding distribution of solar normal

$$S_s = S/\cos\theta = \frac{\pi S_{day}}{2}\sin(\frac{\pi t}{D})/\cos\theta \qquad (2a)$$

and

$$S_s = S/\cos\theta = \frac{\pi S_{day}}{2}\cos(\frac{\theta-\theta_n}{\pi/2-\theta_n}\frac{\pi}{2})/\cos\theta\,. \qquad (2b)$$

Plots of Eq. (2a) and Eq. (2b) at the given conditions of Fig. 1 are represented by curve *d* and curve *e*, respectively. It shows that S_s determined by both of the assumptions reaches the lowest at noon with higher values at sunrise and sunset. This is physically unreasonable and obviously not the case in reality. In ecological models that separate canopy into sunlit and shaded leaves, the sunlit leaf irradiance S_l is directly projected from S_s using a mean leaf-sun angle. Therefore,

using the sine-curve prescription of Eq. (1a) or Eq. (1b) can cause serious problems of large overestimation of radiation and unrealistic diurnal pattern of S_l.

2.1.2 New calculation method

Solar radiation reached on the earth surface includes direct radiation S_{dir} and diffusive radiation S_{dif}. In our new method, we treat these two components separately. The partition of S_{day} into daily mean direct radiation $S_{day,dir}$ and diffusive radiation $S_{day,dif}$ is made by utilizing the following relationship established by Ruth and Chant (1976) according to the radiation data for several years from four stations of the Canada network.

$$\varepsilon = S_{day,dif} / S_{day}$$
$$= \begin{cases} 0.98 & K_T \le 0.1 \\ \max(0.91 + 1.154K_T - 4.936K_T^2 + 2.848K_T^3, 0.15) & K_T > 0.1 \end{cases} \quad (3)$$

where K_T is a parameter equal to $S_{day}/(S_o \cos\theta_o)$ where S_o is the solar constant (=1367 W m^{-2}) and θ_o is the daily average θ. It means that under very cloudy conditions ($K_T \rightarrow 0$), S_{day} is composed of mainly $S_{day,dif}$, but on very clear days ($K_T > 0.6$) larger fraction of S_{day} is $S_{day,dir}$. Similar relationships to Eq. (3) have also been obtained by other authors using different radiation data sets (e.g., Collares-Pereira and Rabl, 1979; Erbs et al., 1982). The separation of S_{day} into $S_{day,dir}$ and $S_{day,dif}$ does not bring extra calculations in ecological models that separate canopy leaves into sunlit and shaded because it is also required in estimating the sunlit and shaded leaf irradiance.

The transmission and attenuation of direct radiation in the atmosphere is mainly determined by the processes of Rayleigh scattering and absorption by ozone, water vapour, and aerosol. Under cloudless conditions, the intensity of direct normal radiation reached on the earth surface $S_{s,dir}$ can be calculated by the product of S_o and the transmittances determined by the various scattering and absorption processes. The integrated transmittance is found closely related to θ. As a result, $S_{s,dir}$ on the earth surface decreases significantly with θ. This has been widely

demonstrated by both observations and model simulations (Iqbal, 1983). Therefore, a more reasonable assumption is that $S_{s,dir}$, rather than S, follows the sine-curve of

$$S_{s,dir} = S_{s,dir,n} \cos(\frac{\theta - \theta_n}{\pi/2 - \theta_n} \frac{\pi}{2}) \tag{4}$$

where $S_{s,dir,n}$ is $S_{s,dir}$ at noon. According to this assumption we have

$$S_{dir} = S_{n,dir} \cos(\frac{\theta - \theta_n}{\pi/2 - \theta_n} \frac{\pi}{2}) \cos\theta / \cos\theta_n \tag{5}$$

where $S_{n,dir}$ is S_{dir} at noon. Integrating Eq. (5) with time in a day gives $S_{day,dir}$

$$S_{day,dir} = \frac{S_{n,dir}}{D} \int_0^D \cos(\frac{\theta - \theta_n}{\pi/2 - \theta_n} \frac{\pi}{2}) \cos\theta / \cos\theta_n \, dt \tag{6}$$

There are difficulties to obtain the analytical solution of Eq. (6) so a numerical method is used to find the relationship between $S_{n,dir}$ and $S_{day,dir}$ which is shown in Fig. 2a. It shows that the ratio of $S_{n,dir}/S_{day,dir}$ is determined by a function of θ_n. It varies between 1.71 and 1.95 when θ_n changes between its maximum and minimum values in a year at our study site. This is different from previous studies using the assumption of Eq. (1a) or Eq. (1b), which gives the ratio independent of θ_n and remains to be a

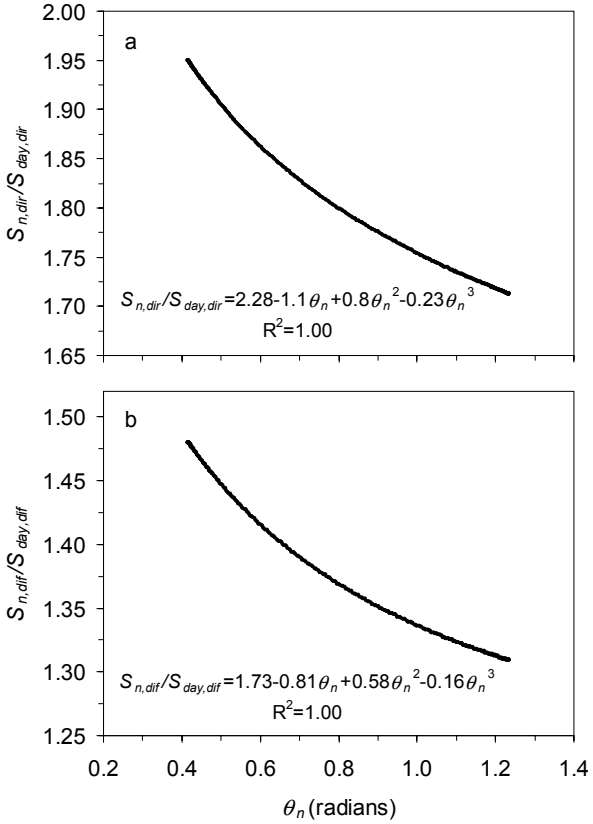

Figure 2. The relationship between the ratio of $S_{n,dir}/S_{day,dir}$ (panel a) and $S_{n,dif}/S_{day,dif}$ (panel b) and daily θ_n. Results are obtained through numerical resolutions of Eq. (6) and Eq. (8). (ϕ=47.3º).

constant of $\pi/2$ (1.57).

The diurnal distribution of S_{dif} is more complicated and does not have the strong geometrical relationships as Eq. (5) for S_{dir}. Under the assumption that diffusive radiation is uniform over the sky dome and weather conditions are relatively stable over time, the diurnal variation of S_{dif} is then mainly affected by θ. Therefore we can simplify the question to

$$S_{dif} = S_{n,dif} \cos(\frac{\theta - \theta_n}{\pi/2 - \theta_n} \frac{\pi}{2}) \tag{7}$$

where $S_{n,dif}$ is S_{dif} at noon. Integrating Eq. (7) with time in a day gives $S_{day,dif}$

$$S_{day,dif} = \frac{S_{n,dif}}{D} \int_0^D \cos(\frac{\theta - \theta_n}{\pi/2 - \theta_n} \frac{\pi}{2}) dt \tag{8}$$

Again, the relationship of $S_{n,dif}$ and $S_{day,dif}$ is obtained through a numerical method (Fig. 2b). The ratio of $S_{n,dif}/S_{day,dif}$ is also related to θ_n and it varies between 1.31 and 1.48 in a year.

With the numerical solutions of Eq. (6) and Eq. (8), we can prescribe the diurnal distribution of S as the sum of S_{dir} (Eq. (5)) and S_{dif} (Eq. (7)). Given the same conditions as in Fig. (1) and a K_T value of 0.8, it is represented by curve *c* in Fig. 1. The normal radiation S_s determined by this new method is represented by curve *f*. It can be found that the diurnal distribution of S_s predicted by our new method is much more theoretically realistic than curve *d* and curve *e* representing the methods widely used in current model applications. Model verifications against measurement will be conducted in Section 3.1.

2.2 Radiation interception of canopy on inclined terrain

2.2.1 Problems with the current calculation method

It is well known that canopy on inclined terrain receives different amount of radiation from that on a horizontal surface. A number of models for estimating topographical solar radiation distribution have been developed in recent years (e.g., Olseth and Skartveit, 1997;

McKenney et al., 1999; Thornton et al., 2000; Tian et al., 2001). These studies mainly focused on the radiation distributions over complex terrain. The interactions between radiation and canopy have been rarely dealt with. For example, the following geometric projection method has been widely used in literatures to deal with the topographic changes of canopy radiation interception (e.g., Garnier and Ohmura, 1968; Swift, 1976; Running et al., 1987; Wigmosta et al., 1994; Sellers et al., 1997)

$$S_c = S\cos\theta_c / \cos\theta \tag{9}$$

where S_c is the solar radiation (or direct solar radiation if S is replaced by S_{dir}) incident on the canopy over inclined terrain and θ_c is the angle between normal to the inclined terrain and sun-earth vector. θ_c is determined by

$$\cos\theta_c = \cos\beta\cos\theta + \sin\beta\sin\theta\cos(\psi - \gamma) \tag{10}$$

where β and γ is the terrain surface slope (inclination from the horizontal position, degrees) and aspect (deviation of the normal to the terrain surface with respect to the local meridian, degrees, south zero, east positive), and ψ is the solar azimuth (degrees, south zero, east positive).

The above calculations can successfully account for the changes of total radiant energy on inclined surfaces. However, we recognise that it is problematic to use S_c obtained by Eq. (9) in modelling ecological processes such as forest photosynthesis. The reason is that whatever the slope and aspect of the terrain is, trees always tend to grow upright. It means that the leaf geometrical positions relative to the solar beam for trees grown on inclined terrain do not differ from that grown on a horizontal surface. Therefore, the radiation intensity incident on plant leaves over inclined terrain should be the same as that over a horizontal surface, at least it is so for the direct component of solar radiation. In other words, the difference of total radiant energy

received by the canopies between inclined and horizontal surfaces is not caused by the change of radiation intensity on canopy leaves.

2.2.2 New calculation method

Direct radiation

Through inspection of the radiation transfer process within the canopy on inclined surfaces, we propose that the topographic change of radiant energy intercepted by canopy is attributed to the variations of sunlit and shaded leaf area index (LAI_{sun} and LAI_{shade}) with topography. LAI_{sun} and LAI_{shade} for a canopy on inclined surfaces can be determined by

$$LAI_{sun} = (1 - e^{-k\Omega LAI/\cos\theta_c})\cos\theta_c / k \tag{11a}$$

$$LAI_{shade} = LAI - LAI_{sun} \tag{11b}$$

where Ω is the foliage clumping index, k is the extinction coefficient, and LAI is the total leaf area index of the canopy. It is worth mention that all of LAI_{sun}, LAI_{shade} and LAI in the above equations are referenced to a unit ground area of the inclined surface. In applications where LAI data are referenced to the horizontal level, the conversion of $LAI_{inclined}=LAI_{horizontal}*\cos(\beta)$ has to be made. It shows that LAI_{sun} and LAI_{shade} changes with the solar beam path within canopy (θ_c) which is determined by the topographic characteristics (Eq. (10)). The direct radiation incident on sunlit leaves $S_{l,dir}$ is then projected using a mean leaf-sun angle θ_l and the direct radiation estimated for horizontal surface (Eq. (5)), rather than the direct radiation on the slope surface obtained in Eq. (9).

$$S_{l,dir} = S_{dir}\cos\theta_l / \cos\theta \tag{12}$$

The sensitivity of leaf physiological activities to radiation intensity can differ greatly from that to the leaf area changes between sunlit and shaded. Therefore, the differentiation of the radiation interception mechanisms discussed above is important in ecological modelling studies.

For example, the light saturation point for most tree species is between 600-1000 μmol m^{-2} s^{-1}, over which leaf photosynthesis increases very little. This number is very often reached under clear weather conditions in summer. Therefore, for the canopy on inclined terrain facing the south, modelling strategy based on the direct geometric projection method (Eq. (9)) which leads to the increase in radiation intensity (when $\beta<\theta_n$) affects the modelled canopy photosynthesis very little. However, due to the large difference of photosynthetic rates between sunlit and shaded leaves, increase in LAI_{sun} caused by the southward inclined terrain according to our new strategy (Eq. (11)) may lead to a significant increase in modelled canopy photosynthesis.

Diffusive radiation

The change of diffusive radiation over the canopy on inclined terrain is caused mainly by two processes, increase of radiation due to the reflection from the surrounding landscape that the inclined terrain "sees" and decrease of sky diffusive radiation due to the decreased sky dome. Formulating these two processes accurately is difficult due to the complex conditions of weather (clear, cloudy, and overcast) and surrounding landscape (distant topography and reflectance properties). By assuming the surrounding landscape has the same albedo α as the subject terrain and the reflectances to direct and diffusive radiation are identical, we can obtain the radiation reflected from the surrounding landscape and incident on the inclined subject terrain, S_r, under the isotropic reflection conditions.

$$S_r = S\alpha(1-\cos\beta)/2\,. \tag{13}$$

Also, under the assumption that sky diffusive radiation is uniform over the sky dome, the sky diffusive radiation incident on the inclined terrain, S_v, can be given by

$$S_v = S_{dif}(1+\cos\beta)/2\,. \tag{14}$$

The ratio of S_{dif} incident on the inclined terrain to that on a horizontal surface, r, is obtained as

$$r = [S\alpha(1-\cos\beta)/2 + S_{dif}(1+\cos\beta)/2]/S_{dif}$$
$$= (1+\cos\beta+\alpha/\varepsilon-\alpha\cos\beta/\varepsilon)/2 \quad (15)$$

where ε is the parameter determined by Eq. (3).

Eq. (15) shows that if the surface albedo α equals to ε, the inclined terrain receives the same amount of diffusive radiation as the horizontal surface (r=1). Field observations show that albedo of the boreal forests is around 0.08 for conifers and 0.15 for deciduous aspen (Betts and Ball, 1997). This number is usually lower than ε under most weather conditions, which results in r<1, indicating that inclined terrain tends to receive lower diffusive radiation than the horizontal surface. However, numerical analyses show that the decrease of diffusive radiation incident on inclined terrain of low to moderate slopes is less than a few percent. Therefore, the impact of topography on S_{dif} is fairly small and can be overlooked in modelling applications.

The intercepted S_{dif} is assumed evenly distributed among the total canopy leaves

$$S_{l,dif} = (S_{dif} - S_{dif,under})/LAI + C \quad (16)$$

where $S_{l,dif}$ and $S_{dif,under}$ is the diffusive radiation on the leaf surface and under the canopy, and C arises from multiple scattering of S_{dir} (Norman, 1982). They are given by

$$S_{dif,under} = S_{dif}e^{-k\Omega LAI} \quad (17)$$

$$C = 0.07\Omega S_{dir}(1.1-0.1LAI)e^{-\cos\theta_c} \quad (18)$$

Since C is θ_c dependent, even with the same S_{dif} over the canopy on complex terrain as that over the horizontal surface, $S_{l,dif}$ can still be different. However, this difference is found fairly small, as can be seen from the model experiment discussed in Section 3.2.

Finally, sunlit leaf irradiance is obtained by $S_{l,dir}$+$S_{l,dif}$ (Eq. (12) and Eq. (16)) and shaded leaf irradiance is $S_{l,dif}$. They can then be used separately for the sunlit and shaded leaf photosynthesis (A_{sun} and A_{shade}) calculations. Total canopy photosynthesis A_c is then scaled up as

$$A_c = A_{sun} LAI_{sun} + A_{shade} LAI_{shade} . \quad (19)$$

3 Model experiment

3.1 Comparison of daily radiation distribution

The new relationship developed in Section 2.1.2 for prescribing the diurnal distribution of solar radiation was compared with measurement as well as the sine-curve methods of Eq. (1a) and Eq.(1b). Fig. 3 gives the results on a typical clear day, in which the dots represent the measured solar radiation at 15min time-intervals at the Old Aspen site (ϕ=53.6°) in the Southern Study Area (SSA-OA) during the BOREAS field campaign in 1994. It shows that the pattern predicted by the method of this study is significantly improved compared with the other two methods. The noon time radiation predicted by the two sine-curves of Eq. (1a) and Eq. (1b) was about 12% lower than that predicted by the method of this study which was very close to the measurement. In the early morning or late afternoon, our new method predicted a concave relationship ($\partial^2 S/\partial t^2>0$). This was found to be consistent with the measurement. On the contrary, both of the sine-curve methods gave a convex relationship ($\partial^2 S/\partial t^2>0$) in the early morning and late afternoon, which led to the overestimation of radiation during that time. Accurate prediction of solar radiation in the early morning and late afternoon is very important because the response of plant

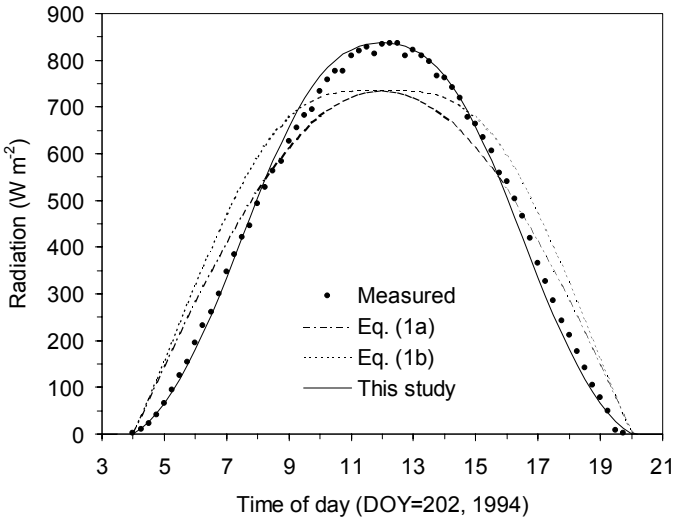

Figure 3. Comparisons of 15min radiation distribution between measured (dots) and predicted using the sine-curve methods of Eq. (1a) (dotted line) and Eq. (1b) (dashed line) and the method of this study (solid line) on a clear day at the SSA-OA site of BOREAS (lat. 53.6ºN, long.106.2ºW).

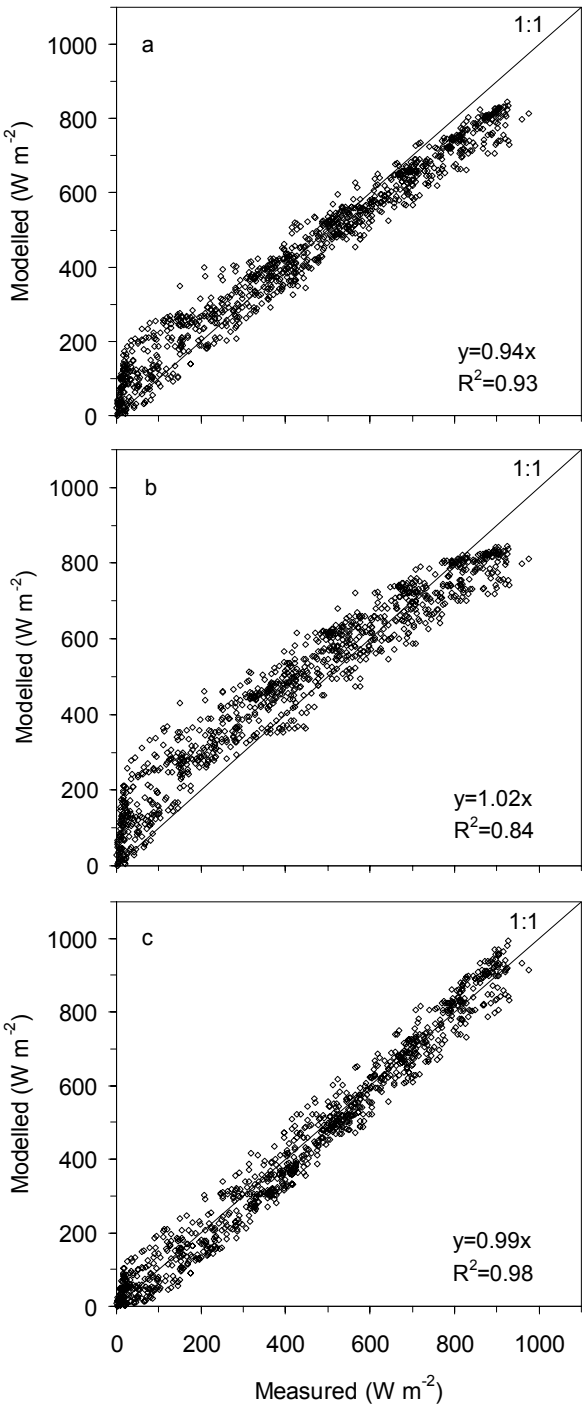

Figure 4. Regression analyses of measured and predicted hourly solar radiation. Panel a, method of Eq. (1a); panel b, method of Eq. (1b); panel c, method of this study. Data shown in the figures are all the clear days (filtered by K_T>0.6) observed in 1999 at the Montmorency ecological station (lat. 47.3ºN, long. 71.1ºW,) in Canada.

photosynthesis to radiation variations is close to a linear relationship at low to middle radiation levels. The overestimation of radiation in the early morning and late afternoon and underestimation around noon by the two sine-curve methods was found on all clear days throughout the year.

In addition, it is worth noting that while our new method and the sine-curve method of Eq.(1a) can correctly predict the daily mean radiation S_{day}, the sine-curve method of Eq.(1b) always gave overestimations. This is because the method to obtain S_{day} by integrating Eq. (1b) with θ (Chen et al., 1999) is theoretically incorrect. In other words, due to the non-linear relationship between time and θ, S_{day} can only be obtained by integrating S in Eq. (1b) with time. Theoretical analysis indicates that the overestimation of S_{day} predicted by integrating S with θ is mainly dependent on θ_n, and it ranges

approximately from 6% on the Summer Solstice to 20% on the Winter Solstice.

Our new calculation method was also tested against radiation measurement from other sites with different latitude. The improvement discussed above was found in all the tests. Fig. 4 gives the regression results between hourly radiation predicted by the three methods and measured at an ecological station located in the Montmorency watershed (ϕ=47.3°), about 100 km north of Quebec City in Canada. Data shown in Fig. 4 include all the clear days in 1999 filtered by K_T>0.6. The overestimation at low radiation levels and underestimation at high radiation levels is obvious in Fig. 4a, predicted by the sine-curve method of Eq. (1a), and in Fig. 4b, predicted by the sine-curve method of Eq. (1b). While in Fig. 4c predicted by the method of this study, no systematic deviation from the 1:1 line was found. The correlation coefficient (R^2) between the model predicted and measured hourly solar radiation in the above clear days was 0.93, 0.84, and 0.98 for the modelling methods of Eq (1a), Eq. (1b) and this study, respectively. After including all the days in the year that had various weather condition, the above R^2 changed to 0.86, 0.81, and 0.88, respectively. Therefore, it can be concluded that both of the sine-curve methods not only can cause serious problems in the modelling strategy of separating canopy leaves into sunlit and shaded (discussed in Section 2.1.1), they also face accuracy limitations when applied in simple models such as using radiant energy and light use efficiency for photosynthesis estimations.

Liu (1996) compared radiation measurement with three approximations of diurnal radiation distribution with time, namely constant, triangular, and sine-curve. It was found that the triangular method overestimated the noon peak values of radiation and the sine-curve method underestimated the noon peak values on clear days. He also evaluated the effects of the three approximations on calculating daily photosynthesis. It was indicated that the triangular method

was most reliable among the three approaches. Root mean square error of daily A_c predicted by the triangular method was only half of that predicted by the sine-curve method. It was also found that the large error by the sine-curve method was mainly attributed to the higher values predicted in the early morning and late afternoon caused by the overestimates of radiation during that time. The pattern of solar radiation obtained from our study is between the triangular and sine-curve predictions in Liu's study, and our modelled results are consistent with his experiment.

3.2 Topography and radiation interception of canopy

According to our hypothesis in Section 2.2.2, topography affects canopy interception of direct radiation through altering LAI_{sun} and LAI_{shade} (Eq. (11)) and diffusive radiation through affecting the multiple scattering of direct radiation within the canopy (Eq. (18)). Both of the processes are controlled by θ_c determined by the position of the sun (zenith and azimuth) and the local topographic slope and aspect (Eq. (10)). In the model experiment discussed below (also in Section 3.3), the following parameter values typical for a clear day during growing season in the Canadian boreal forest region were used: ϕ=50° N, DOY=215, S_n=800 W m^{-2}, ε=0.2, conifer land cover with LAI=6.0 m^2 m^{-2}, Ω=0.5, θ_l=60°, and k=0.5.

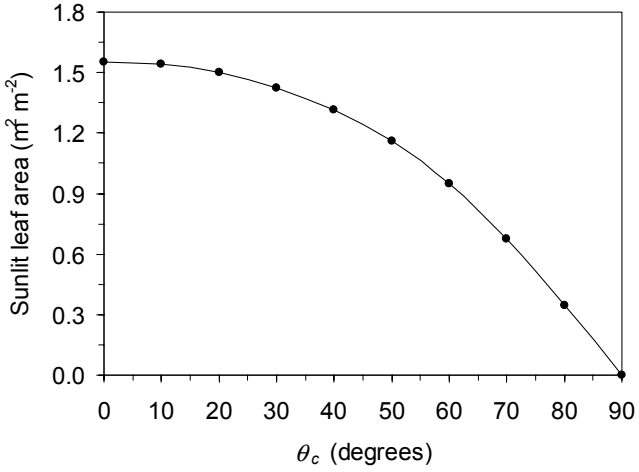

Figure 5. Variations of simulated sunlit leaf area index with the incidence angle of solar beam with respect of canopy surface. (LAI=6.0 and Ω =0.5).

The simulated relationship between LAI_{sun} and θ_c is shown in Fig. 5. Variations of θ_c changed the beam path within canopy, leading to the changes of shadowed area of sunlit leaves.

As a result, LAI_{sun} decreased with the increase of θ_c and this variation was more significant when θ_c was high. The modelled maximum LAI_{sun} was 1.55 at θ_c=0. According to Eq. (11), the maximum LAI_{sun} of a canopy has an upper limit of 2.0 under any kinds of conditions.

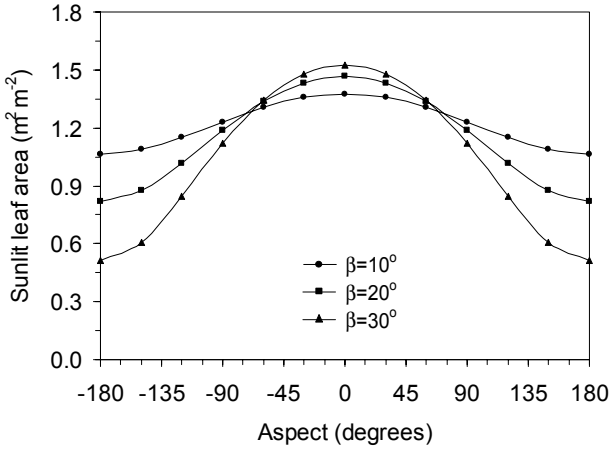

Figure 6. Variations of simulated sunlit leaf area index with topographic aspect under three different slopes (10º, 20º, and 30º). (ϕ=47.3º, DOY=129, *LAI*=6.0, and Ω =0.5).

The impact of topography on LAI_{sun} was investigated by applying the above relationship to assumed land surfaces with different slopes and aspects (Fig. 6). There was no topographic shadowing effect considered. Under $\beta \leq \theta_n$, the south facing terrain (γ=0) was modelled to have the highest LAI_{sun} and the north facing terrain (γ=±180) have the lowest LAI_{sun}. The variation of LAI_{sun} with γ was smaller if the slope was lower. For example, under the given conditions and with a slope of 10°, LAI_{sun} of south facing terrain was modelled about 27% higher than that of north facing terrain (1.4 vs. 1.1 m^2 m^{-2}). While with a slope of 30°, LAI_{sun} of south facing terrain was modelled three times higher than that of north facing terrain (1.5 vs. 0.5 m^2 m^{-2}).

Since direct radiation received by sunlit leaves was modelled the same for plants over any kinds of topography, the total amount of direct radiation intercepted by canopy was solely controlled by LAI_{sun}. Therefore, the impact of topography on the canopy interception of S_{dir} (solid lines in Fig. 7) had the similar patterns with that of topography-LAI_{sun} (Fig. 6). The total intercepted PPFD (photosynthetic photon flux density, calculated by assuming the visible shortwave radiation fraction =0.5 and PPFD-energy ratio =4.55 μmol J^{-1}) of south facing terrain

with a slope of 30° was modelled at 690 μmol m^{-2} s^{-1}, which was three times higher than that of north facing terrain with the same slope. The topographic distribution of the intercepted S_{dir} by canopy obtained from our calculation method was the same as that obtained from the direct geometric projection approach (Eq. (9)). However, it was due to the variation of LAI_{sun} that contributed to topographic change in our model, rather than the topographic difference in radiation intensity according to Eq. (9). This differentiation in the interception mechanisms of S_{dir} can lead to significant differences in modelled photosynthesis (discussed in Section 3.3).

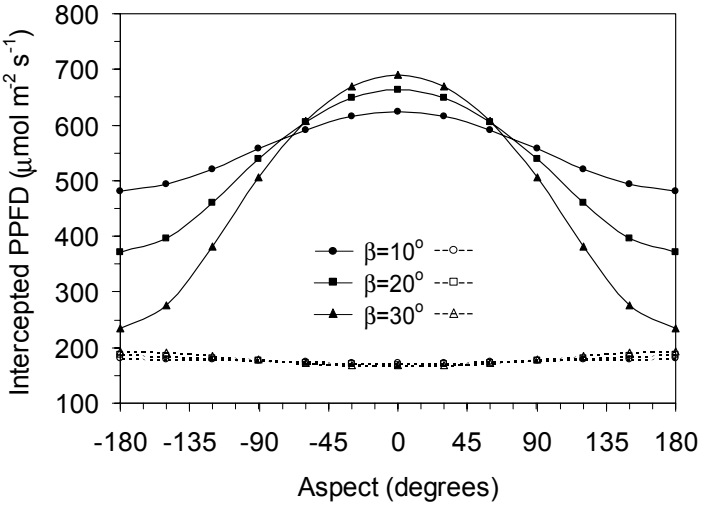

Figure 7. Topographic variations of canopy intercepted direct (solid lines) and diffusive (dotted lines) radiation simulated with the same parameters as in Figure 6.

The intercepted S_{dif} by canopy changed slightly with topographic slopes and aspects (dashed lines in Fig. 7). Decrease in the multiple scattering of S_{dir} within canopy with θ_c (Eq. (18)) caused the slightly lower interception of S_{dif} for south facing terrain or with smaller slopes. But these variations were very small and within 25 μmol m^{-2} s^{-1} among the examples in Fig. 7.

3.3 Topography and canopy photosynthesis

By using the same site parameters as in Section 3.2, photosynthesis was calculated according to the BEPS model (Chen et al., 1999). It describes the leaf gross photosynthesis rate of C3 plants as the minimum of light-limited and Rubisco-limited reaction rates, following the approach proposed by Farquhar et al. (1980). Canopy photosynthesis was then scaled up from

sunlit and shaded leaf calculations according to Eq. (19). To investigate topographic impacts of radiation on A_c, we focused our discussions on the light reaction rate where radiation plays the determining role in photosynthesis. Other assumptions included an optimum air temperature of 25°C and light-saturated rate of electron transport J_{max}=50 μmol m^{-2} s^{-1}.

Though the two calculation methods discussed in Section 3.2 gave the same amount of total radiant energy interception for a given site, A_c obtained from them was different (Fig. 8). The most prominent characteristic was that the topographic variations of A_c obtained from our method (solid lines) were remarkably higher than that obtained from the geometric projection method (dashed lines). For example, with the same slope of 30°, A_c modelled using our method was as high as 13.3 μmol m^{-2} s^{-1} for south facing terrain and as low as 9.7 μmol m^{-2} s^{-1} for north facing terrain, while the corresponding numbers obtained from the geometric projection method were 12.5 vs. 11.2 μmol m^{-2} s^{-1}. Reasons for this difference were that according to our new method, it was LAI_{sun}, rather than the radiation intensity on leaf surface as in the geometric projection method, that changed with topography. While A_c had the linear relationship with LAI_{sun} (Eq. (19)) which changed substantially with topography (Fig. 6), it changed with radiation following the Michaelis-Menten equation in the model by which it was insensitive to radiation at high radiation levels. As a result, on clear days with high solar

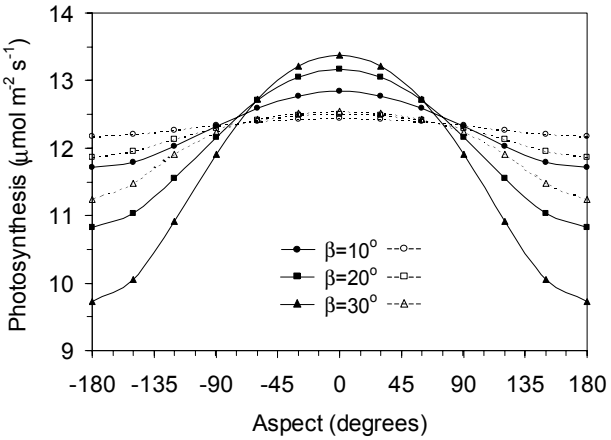

Figure 8. Topographic variations of light-limited canopy photosynthesis simulated by using the geometric projection approach (dotted lines) and the scheme of this study (solid lines) in radiation

radiation, the topographic variations of A_c obtained from the geometric projection approach were greatly depressed.

For a given slope, the increase of A_c on those sites facing southward can not compensate the decrease on those sites facing northward. For example, compared with A_c modelled on a horizontal surface (12.34 μmol m^{-2} s^{-1}), it was increased 8% on a 30° slope facing south and decreased 21% on the same slope but facing north. As a result, the spherically integrated A_c with aspect (-180° - +180°) tended to decrease when the landscape becomes undulate. For terrain with slopes of 10°, 20°, and 30°, the integrated A_c was modelled at 12.25, 11.99, and 11.57 μmol m^{-2} s^{-1}, respectively, slightly lower than that on the horizontal surface. These results also suggest that for model regional applications, if the mean spherical slope and aspect of a grid is close to zero, the impact of sub-grid landscape variations below the model resolution on the overall estimate of the total grid A_c is very limited (<5% for most cases).

4 Discussion and conclusions

Radiation calculations play important roles in modelling studies of terrestrial ecosystems. The results of this study indicate that both of the sine-curve assumptions of diurnal solar radiation variation with time (Eq. (1a)) and with solar zenith angle (Eq. (1b)) lead to unreasonable pattern of solar normal radiation. Therefore they are not appropriate to the model applications that separate canopy leaves into sunlit and shaded. The new calculation method developed in this study can not only give a reasonable distribution pattern of solar normal radiation (Fig. 1), it also gives higher prediction accuracy (Fig. 3 and Fig. 4). A valuable application of the approach is for filling missing observations or extrapolating daily data to hourly values so that the short time step models can be investigated when only daily observation is available. This study also indicates that the widely used geometrical projection method is not

physically realistic to calculate canopy radiation interceptions over complex terrain. A better scheme is attributing the topographic effects on radiation interceptions of canopy to the changes of sunlit and shaded leaf area index. The two new approaches proposed in this study are found more physically realistic in regenerating the natural processes than the approaches currently used in most models. These improvements can help models address the ecosystem energy, water and carbon simulations more accurately. They also benefit the temporal integration studies and the spatial scale analysis over complex terrain.

Model experiment on canopy photosynthesis shows that its topographic variations predicted by using the new radiation interception scheme are very significant and higher than that predicted by using the geometrical projection approach, implying the necessities of including topographic impacts in model regional applications at high spatial resolution. It also indicates that the variations of spherically integrated canopy photosynthesis are small (within a few percent) among different terrain slops and they are close to that obtained for a horizontal surface. This suggests that photosynthesis of a region can be estimated with the absent of topographic details if it is of a spherical mean slope and aspect close to zero. In other words, topographic impacts play less important roles in model applications at low spatial resolutions due to the topographic averaging effects within pixels.

Many factors determine plant photosynthesis over complex terrain. The bottleneck factor can be very different in different ecosystems, such as soil moisture in arid eco-regions and temperature in boreal eco-regions. This study focused on the topographic radiation impacts only. The spatial variations of vegetation (e.g., *LAI*, vegetation species, and tree ages), soil (e.g., moisture, nutrient conditions), and microclimate (e.g., topographic difference in temperature) conditions were not included, which may limit the applications of our modelled results. For

instance, *LAI* directly determines the canopy radiation interception and photosynthetic rates. Its spatial variation can greatly affect the areal distribution of modelled photosynthesis. It is possible that the topographic variation of canopy photosynthesis found in this study becomes more or less pronounced under different spatial patterns of *LAI*, or even more, the model runs the risk of biased predictions by using averaged parameters and driving variables. The same situation applies to the spatial variations of all other variables such as soil water content. The biases found in some model studies by using area-averaged parameters in regional estimation (e.g., Band, 1993; Pierce and Running, 1995) may be partially attributed to the consideration of spatial vegetation and soil water information. In addition, a high *LAI* value of 6.0 m^2 m^{-2} was used in our model experiment. Since the variation of canopy radiation interception is less sensitive to *LAI* in high *LAI* values than in low *LAI* values, a more pronounced topographic distribution of canopy photosynthesis can be expected if canopy *LAI* varies in lower values.

Acknowledgements

We thank Dr. T.A. Black of University of British Columbia and Dr. P.Y. Bernier of Laurentian Forestry Centre of Canadian Forest Service for the permission to use the radiation measurement included in this paper. We are grateful to Sylvain Leblanc of Canadian Centre for Remote Sensing for his interest and internal review of the manuscript.

Nomenclature

Ω	foliage clumping index
ε	fraction of diffusive radiation in total solar radiation
ψ	solar azimuth (south zero, east positive)
γ	terrain surface aspect (south zero, east positive)
β	terrain surface slope (inclination from horizontal position)
α	albedo
ϕ	latitude
θ	solar zenith angle
θ_c	angle between normal to the inclined terrain and sun-earth vector
θ_l	mean leaf-sun angle
θ_n	θ at noon
θ_o	daily average θ
A_c	canopy photosynthesis
A_{shade}	shaded leaf photosynthetic rate
A_{sun}	sunlit leaf photosynthetic rate
C	multiple scattering of S_{dir} within canopy
D	day length
DOY	Julian day of the year
k	extinction coefficient
K_T	parameter, $=S_{day}/(S_o \cos\theta_o)$
LAI	total leaf area index of canopy
LAI_{shade}	shaded leaf area index

LAI_{sun}	sunlit leaf area index
S	instantaneous solar radiation on a horizontal surface
S_c	solar radiation incident on canopy over inclined terrain
S_{day}	daily mean S
$S_{day,dif}$	daily mean diffusive radiation
$S_{day,dir}$	daily mean direct radiation
S_{dif}	diffusive solar radiation
$S_{dif,under}$	diffusive solar radiation under canopy
S_{dir}	direct solar radiation
S_l	radiation on leaf surface
$S_{l,dif}$	diffusive radiation on leaf surface
$S_{l,dir}$	direct radiation on leaf surface
S_n	S at noon
$S_{n,dif}$	S_{dif} at noon
$S_{n,dir}$	S_{dir} at noon
S_o	solar constant
S_r	S reflected from surrounding landscape and incident on inclined terrain
S_s	solar normal radiation
$S_{s,dir}$	direct normal radiation
$S_{s,dir,n}$	$S_{s,dir}$ at noon
S_v	diffusive radiation incident on inclined terrain
t	time

References

Band, L.E., 1993. Effects of land surface representation on forest water and carbon budgets. J. Hydrol. 150, 749-772.

Betts, A.K., Ball J.H., 1997. Albedo over the boreal forest. J. Geophy. Res. 102 (D24), 28,901-28909.

Boote, K.J., Loomis, R.S., 1991. The prediction of canopy assimilation. In: Boote, K.J., Loomis, R.S. (Eds), Modelling Crop Photosynthesis from Biochemistry to Canopy, vol. 19. pp. 109-140. CSSA, Madison, Wisconsin, USA.

Chen, J.M., Liu, J., Cihlar, J., Goulden, M.L., 1999. Daily canopy photosynthesis model through temporal and spatial scaling for remote sensing applications. Ecol. Model. 124, 99-119.

Collarse-Pereira, M., Rabl, A., 1979. The average distribution of solar radiation correlations between diffusive and hemispherical and between daily and hourly insolation value. Sol. Energy 22, 155-164.

Erbs, D.G., Klein, S.A., Duffie, J.A., 1982. Estimation of the diffusive radiation fraction for hourly, daily and monthly-average global radiation. Sol. Energy 28, 293-302.

Farquhar, G.D., von Caemmerer, S., Berry, J.A., 1980. A biochemical model of photosynthetic CO_2 assimilation in leaves of C3 species. Planta 149, 78-90.

Garnier, B.J., Ohmura, A., 1968. A method of calculating the direct shortwave radiation income of slopes. J. Appl. Meteorol. 7, 796-800.

Hanson, J.D., 1991. Analytical solution of the rectangular hyperbola for estimating daily net photosynthesis. Ecol. Model. 58, 209-216.

Iqbal, M., 1983. An introduction to solar radiation. Academic Press, Canada.

Liu, D.L., 1996. Incorporating diurnal light variation and canopy light attenuation into analytical equations for calculating daily gross photosynthesis. Ecol. Model. 93, 175-189.

Liu, J., Chen, J.M., Cihlar, J., Park, W.M., 1997. A processed-based boreal ecosystem productivity simulator using remote sensing inputs. Remote Sens. Environ. 62, 158-175.

McGuire, A.D., Melillo, J.M., Kicklighter, D.W., Pan, Y., Xiao, X., Helfrich, J., Moore III, B., Vörösmarty, Schloss, A.L., 1997. Equilibrium responses of global net primary production and carbon storage to doubled atmospheric carbon dioxide: sensitivity to changes in vegetation nitrogen concentration. Global Biogeochem. Cycles 11, 173-189.

McKenney, D.W., Mackey, B.G., Zavitz, B.L., 1999. Calibration and sensitivity analysis of a spatially-distributed solar radiation model. Int. J. Geographical Information Sci. 13, 49-65.

Monteith, J.L., 1965. Light distribution and photosynthesis in field crops. Ann. Bot. 29, 17-37.

Norman, J.M., 1982. Simulation of microclimates. In: Hatfield, J.L., Thomason, I.J. (Eds.), Biometeorology in Integrated Pest Management, Academic Press, New York, pp. 65-99.

Olseth, J.A. and Skartveit, A., 1997. Spatial distribution of photosynthetically active radiation over complex topography. Agric. For. Meteorol. 86, 205-214.

Parton, W.J., Schimel, D.S., Cole, C.V., Ojima, D.S., 1987. Analysis of factors controlling soil organic matter levels in Great Plains grasslands. Soil Sci. Soc. Am. J. 51, 1173-1179.

Pierce, L.L., Running, S.W., 1995. The effects of aggregating sub-grid land surface variation on large-scale estimates of net primary production. Landscape Ecol. 10, 239-253.

Running, S.W., Nemani, R.R., Hungerford, R.D., 1987. Extrapolation of synoptic meteorological data in mountainous terrain and its use for simulating forest evapotranspiration and photosynthesis. Can. J. For. Res. 17, 472-483.

Running, S.W., Coughlan, J.C., 1988. A general model of forest ecosystem processes for regional applications. I. Hydrologic balance, canopy gas exchange and primary production processes. Ecol. Model. 42, 125-154.

Ruth, D.W., Chant, R.E., 1976. The relationship of diffusive radiation to total radiation in Canada. Sol. Energy 18, 153-154.

Sands, P.J., 1995. Modelling canopy production. II. From single-leaf photosynthetic parameters to daily canopy photosynthesis. Aust. J. Plant Physiol. 22, 603-614.

Sellers, P.J., Heiser, M.D., Hall, F.G., Verma, S.B., Desjardins, R.L., Schuepp, P.M., MacPherson, J.I., 1997. The impacct of using area-averaged land surface properties-topography, vegetation condition, soil wetness-in calculations of intermediate scale (approximately 10 km2) surface-atmosphere heat and moisture fluxes. J. Hydrol. 190, 269-301.

Sinclair, T.R., Knoerr, K.R., 1982. Distribution of photosynthetically active radiation in the canopy of a loblolly pine plantation. J. Appl. Ecol. 19, 183-191.

Swift, L.W., 1976. Algorithm for solar radiation on mountain slopes. Water Resour. Res. 12, 108-112.

Thornton, P.E., hasenauer, H., and White, M.A., 2000. Simultaneous estimation of daily solar radiation and humidity from observed temperature and precipitation: an application over complex terrain in Austria. Agric. For. Meteorol. 104, 255-271.

Tian, Y.Q., Davies-Colley, R.J., Gong, P., and Thorrold, B.W., 2001. Estimating solar radiation on slopes of arbitrary aspect. Agric. For. Meteorol. 109, 67-74.

Wang, S.S., Grant, R.F., Verseghy, D.L., Black, T.A., 2001. Modelling plant carbon and nitrogen dynamics of a boreal aspen forest in CLASS – the Canadian Land Surface Scheme. Ecol. Model. 142, 135-154.

Wang, S., Grant, R.F., Verseghy, D.L., and Black, T.A., 2002. Modelling carbon-coupled energy and water dynamics of a boreal aspen forest in a GCM land surface scheme. *Int. J. Climatol*., (in press).

Wigmosta, M.S., Vail, L.W., Lettenmaier, D.P., 1994. A distributed hydrology-vegetation model for complex terrain. Water Resour. Res. 30, 1665-1679.